HHS Public Access

Author manuscript

Sci Transl Med. Author manuscript; available in PMC 2020 November 17.

Published in final edited form as:

Sci Transl Med. 2014 December 24; 6(268): 268ra177. doi:10.1126/scitranslmed.3009961.

Recurrent epimutation of *SDHC* in gastrointestinal stromal tumors

J. Keith Killian[1], **Markku Miettinen**[2], **Robert L. Walker**[1], **Yonghong Wang**[1], **Yuelin Jack Zhu**[1], **Joshua J. Waterfall**[1], **Natalia Noyes**[1], **Parvathy Retnakumar**[1], **Zhiming Yang**[2], **William I. Smith Jr.**[3], **M. Scott Killian**[4], **C. Christopher Lau**[1], **Marbin Pineda**[1], **Jennifer Walling**[1], **Holly Stevenson**[1], **Carly Smith**[5], **Zengfeng Wang**[2], **Jerzy Lasota**[2], **Su Young Kim**[6], **Sosipatros A. Boikos**[6], **Lee J. Helman**[6], **Paul S. Meltzer**[1,*]

[1]Genetics Branch, National Cancer Institute, National Institutes of Health (NIH), Bethesda, MD 20892, USA

[2]Laboratory of Pathology, Center for Cancer Research, NIH, Bethesda, MD 20892, USA

[3]Department of Pathology, Suburban Hospital, Bethesda, MD 20814, USA

[4]University of South Dakota, Vermillion, SD 57069, USA

[5]National Heart Lung and Blood Institute, NIH, Bethesda, MD 20892, USA

[6]Pediatric Oncology Branch, Center for Cancer Research, NIH, Bethesda, MD 20892, USA

Abstract

Succinate dehydrogenase (SDH) is a conserved effector of cellular metabolism and energy production, and loss of SDH function is a driver mechanism in several cancers. SDH-deficient gastrointestinal stromal tumors (*d*SDH GISTs) collectively manifest similar phenotypes, including hypermethylated epigenomic signatures, tendency to occur in pediatric patients, and lack of *KIT/PDGFRA* mutations. *d*SDH GISTs often harbor deleterious mutations in SDH subunit genes *(SDHA, SDHB, SDHC,* and *SDHD,* termed *SDHx),* but some are *SDHx* wild type (WT). To further elucidate mechanisms of SDH deactivation in *SDHx*-WT GIST, we performed targeted exome sequencing on 59 *d*SDH GISTs to identify 43 *SDHx*-mutant and 16 *SDHx*-WT cases. Genome-wide DNA methylation and expression profiling exposed *SDHC* promoter–specific CpG island hypermethylation and gene silencing in *SDHx*-WT *d*SDH GISTs [15 of 16 cases (94%)]. Six of 15 *SDHC*-epimutant GISTs occurred in the setting of the multitumor syndrome Carney triad. We observed neither *SDHB* promoter hypermethylation nor large deletions on chromosome 1q in any *SDHx*-WT cases. Deep genome sequencing of a 130-kbp (kilo–base pair) window

*Corresponding author. pmeltzer@mail.nih.gov.

Author contributions: Designed and performed experiments: J.K.K., M.M., R.L.W., J.J.W., N.N., P.R., Z.Y., W.I.S.J., C.C.L., M.P., J.W., H.S., C.S., Z.W., J.L., S.Y.K., S.A.B., L.J.H., and P.S.M.; analyzed data: J.K.K., M.M., Y.W., Y.J.Z., W.I.S.J., M.S.K., S.Y.K., S.A.B., L.J.H., and P.S.M.; wrote the paper: J.K.K., M.M., W.I.S.J., M.S.K., L.J.H., and P.S.M.

Competing interests: The authors declare that they have no competing interests.

Data and materials availability: The original gene expression data shown in this publication have been deposited in the NCBI (National Center for Biotechnology Information) GEO and are accessible through GEO Series accession no. GSE56670.

SUPPLEMENTARY MATERIALS

www.sciencetranslationalmedicine.org/cgi/content/full/6/268/268ra177/DC1

around *SDHC* revealed no recognizable sequence anomalies in *SDHC*-epimutant tumors. More than 2000 benign and tumor reference tissues, including stem cells and malignancies with a hypermethylator epigenotype, exhibit solely a non-epimutant *SDHC* promoter. Mosaic constitutional *SDHC* promoter hypermethylation in blood and saliva from patients with *SDHC*-epimutant GIST implicates a postzygotic mechanism in the establishment and maintenance of *SDHC* epimutation. The discovery of *SDHC* epimutation provides a unifying explanation for the pathogenesis of *d*SDH GIST, whereby loss of SDH function stems from either *SDHx* mutation or *SDHC* epimutation.

INTRODUCTION

The multimeric respiratory complex II/succinate dehydrogenase (SDH)/succinate ubiquinone oxidoreductase (SQR) is an integral component of both the mitochondrial Krebs cycle and respiratory chain [reviewed in (1)], and its four protein subunits (SDHA, SDHB, SDHC, and SDHD) are encoded by nuclear genes. Mutational inactivation of SDH is a tumor mechanism in several tumors including gastrointestinal stromal tumor (GIST), the most common mesenchymal tumor of the gastrointestinal tract. SDH deficiency is typically associated with gastric GIST in pediatric patients, leading to the term “pediatric” GIST, but it also occurs in adults as an alternative mechanism to driver mutations of signal transduction kinases such as *KIT.*

Several studies link disabled SDH function to tumorigenesis through pathologic activation of an otherwise physiologic hypoxia-inducible pathway of angiogenesis, glycolysis, and cell proliferation (2–5), as well as through nuclear epigenomic remodeling due to deranged Krebs cycle function (6–8). Maintenance of epigenomic integrity requires SDH-dependent catalysis of succinate to fumarate. The dioxygenasefamily histone lysine demethylases (containing a jumonji C domain) and the 5-methylcytosine (5mC)–modifying enzymes in the TET family depend on the succinate/α-ketoglutarate (αKG) ratio for proper function. Pathologic elevation of the succinate/αKG ratio (secondary to SDH dysfunction) creates a “pseudo-hypoxic” state mirroring a physiologic response to hypoxia by inhibition of the oxygen-sensing prolyl hydroxylase. This triggers the hypoxia-inducible factor 1α–mediated hypoxia response, whose sequelae in *d*SDH GIST include highly vascularized, hypercellular tumors. Disruption of oxidative demethylation of 5mC due to inhibitory metabolites that accumulate in tumors with mutations in core metabolic pathways may be a mechanism of global DNA hypermethylation common to *d*SDH GIST and paraganglioma (7–9) and to isocitrate dehydrogenase (*IDH*)– and fumarate hydratase (*FH*)–mutant tumors of mesenchymal, epithelial, glial, myeloid, and renal (8, 10–13) lineages. Along with the distinctive genome-wide CpG hypermethylation in *d*SDH GIST relative to *KIT* mutants (7), these tumors also exhibit elevated *IGF1R* gene expression (14–16), which is of potential therapeutic interest.

Biallelic mutation of one of the four SDH component genes—*SDHA, SDHB, SDHC,* or *SDHD* (termed *SDHx*)—often explains SDH deactivation in *d*SDH GIST, because loss of function of any one of the four subunits is sufficient to disrupt the complex, evidenced by an SDHB-negative immunophenotype in histologic tumor tissue sections [reviewed in (1)].

However, a notable proportion of *d*SDH GISTs lack identifiable *SDHx* mutations; the absence of recurrent genomic copy number aberrations or loss of heterozygosity (LOH) events has thus far thwarted efforts to localize a genetic aberration that could disable the SDH complex and explain the pathologic convergence with tumors driven by *SDHx* mutation (17, 18).

Rare patients with *d*SDH GIST may develop additional tumors including paraganglioma and pulmonary chondroma, resulting in a clinical diagnosis of Carney triad, a nonfamilial multitumor syndrome whose genetic basis is unknown and for which no specific clinical tests exist (18). It was originally reported that the most frequent and greatest contiguous change in Carney triad tumors is large genomic deletion on 1q encompassing *SDHC* (19); however, this genomic alteration has not been observed in other studies of *d*SDH GIST [reviewed in (1)]. To fully dissect the molecular basis of SDH deficiency, a comprehensive molecular analysis of a large number of SDH-deficient GISTs, not limited to candidate genes and unselected for Carney triad or *SDHx*-mutation status, is required.

Beyond coding sequence mutations of disease target genes, epigenetic modes of gene inactivation are increasingly recognized. Some examples of these include *MLH1* and *MSH2* silencing via promoter hypermethylation in Lynch syndrome (20) and *FMR1* promoter hypermethylation and silencing in fragile X syndrome (21). In these instances, expression and promoter DNA methylation of the causative gene are abnormal despite a lack of protein-altering mutations; moreover, these patients often exhibit epimutation in their normal somatic tissues.

In the current study, we examined the genomes, methylomes, gene expression profiles, and *SDHx* mutation status of a cohort of 59 *d*SDH GIST patients. Molecular profiling methods were adapted to routinely processed formalin-fixed, paraffin-embedded (FFPE) surgical pathology specimens to maximize patient inclusion, as well as to perform histology-guided tumor dissection for nucleic acid extraction. These analyses uncovered a recurrent gene silencing epimutation highly specific to *SDHx*-WT *d*SDH GIST, encompassing a subset of cases with manifestations of Carney triad. To distinguish between primary and secondary epimutation, we analyzed the cases for potentially causal cis-acting genomic anomalies. Finally, patient blood and saliva were examined for constitutional epimutation to gauge its developmental timing.

RESULTS

SDHx-mutant versus *SDHx*-WT subgroups of *d*SDH GIST

Fifty-nine SDH-disabled (*d*SDH) GIST cases from the National Institutes of Health (NIH) Pediatric GIST clinic were analyzed in this study (Table 1). Cases were selected on the basis of SDHB-negative immunophenotype by immunohistochemistry, a sensitive and specific marker for SDH deficiency (22). SDH deficiency was further confrmed in all tumors by genomic hypermethylation (Table 1 and fig. S1), a molecular hallmark present in all analyzed SDH-deficient GISTs that distinguishes these tumors from *KIT/PDGFRA*– and other kinase pathway-mutant GISTs with intact SDH function (7). Beyond immunophenotypic and molecular epigenomic confirmation of SDH deficiency, the only

other inclusion criterion was sufficient available specimen for genomic DNA (gDNA) library construction for *SDHx* sequencing. Thus, the analyzed set of 59 GISTs represents a comprehensive cross section of SDH-deficient cases. In addition to tumor SDH deficiency, other patient annotations included age at diagnosis, sex, and whether there was a clinical diagnosis of Carney triad (Table 1).

Fifty-nine *d*SDH GIST cases were tested for *SDHx* coding sequence mutations by OncoVar-GIST, a custom-capture single-molecule next-generation DNA sequencing assay (NGS), performed in a Clinical Laboratory Improvement Amendments (CLIA)-certified laboratory, that sequences the complete coding sequence of *SDHA*, *SDHB*, *SDHC*, and *SDHD* from FFPE tissue after tumor dissection by a pathologist. In addition to histology-targeted dissection of tumor tissue, the fraction of malignant cells represented in tumor tissue DNA extracts was empirically calculated from the methyl deviation index (MDI), a quantitative measurement of tumor cell fraction derived from tumor-specific methylated allele frequency in tissue DNA extracts (7, 23). By these measures, all tumor extracts consisted of at least 50% malignant cells and had a median malignant cellularity of greater than 80% according to the MDI metric (Table 1 and fig. S1).

Forty tumors were positive for *SDHx* coding sequence mutation by the OncoVar-GIST sequencing assay, and three additional tumors had intragenic deletions by copy number and/or genotyping microarray (Table 1). A “second hit” leading to biallelic *SDHx* inactivation was demonstrated in 35 of 43 (81%) of *SDHx*-mutant tumors (Table 1 and fig. S2), consistent with the Knudson two-hit model of tumor suppressor gene inactivation (24). The eight instances of *SDHx*-mutant GIST without detection of a second hit were *SDHA* mutants (Table 1). As will be shown further below, these cases did not harbor *SDHA* promoter methylation. Despite the lack of LOH in these *SDHA*-mutant GISTs, four of them had loss of SDHA protein expression by immunohistochemistry, a biomarker of deleterious *SDHA* mutation in GIST (25). Beyond these exceptions to the two-hit model, all other *SDHA*-mutant GISTs ($n = 17$) harbored second hits. Thus, overall, the 59 *d*SDH GIST cases were split into the *SDHx*-mutant ($n = 43$) and *SDHx*-WT ($n = 16$) groups (Table 1). Regarding clinical molecular testing for *SDHx* mutation in GIST, our laboratory’s analyses suggest that up to one of three of SDH-deficient GISTs (16 of 59) lack sequence mutations in *SDHx*, a frequency that has not been well documented previously.

SDHC promoter hypermethylation in *SDHx*-WT GIST

The DNA methylomes of 59 individual *d*SDH GISTs were profiled by Illumina 450K Infinium methylation beadarray [Gene Expression Omnibus (GEO) platform GPL13534]. In a *t*-test two-group comparison of *SDHx*-WT versus *SDHx*-mutant tumors, the methylation levels of 11 CpG targets (of 485,577 total) demonstrated significant hypermethylation ($q < 0.05$) in *SDHx*-WT GIST (Fig. 1A). All 11 targets mapped to a 656–base pair (bp) genomic interval encompassing the two *SDHC* promoter CpG islands (CGIs) on chromosome 1q23.3 (Fig. 1B). Outside the *SDHC* promoter, there was no significant ($q < 0.05$) CpG target hypermethylation elsewhere in the *SDHx*-WT GIST genome (Fig. 1A), including *SDHA, SDHB,* and *SDHD* (fig. S3). Although all hypermethylated targets mapped to the *SDHC* promoter, scattered CpG targets registered as significantly hypomethylated ($q < 0.05$), yet

were close to the border of statistical significance (fig. S4); future studies on additional *SDHx*-WT tumors may further clarify the biological relevance, if any, of these hypomethylated targets to pathogenesis.

We next categorized the zygosity (homozygous versus heterozygous) of *SDHC* promoter methylation in *SDHC*me tumors for correspondence with *SDHx* mutation status. Because the malignant cell fraction in tumors may be expected to influence the measurement of *SDHC* promoter–methylated alleles in whole tumor extracts (the nonnormalized *SDHC*me allele frequency), tumor *SDHC* promoter methylation was normalized to malignant cell fraction in tumor lysates to derive the tumor *SDHC*me zygosity index *(SDHC* promoter–methylated allele frequency normalized to tumor malignant cell purity). Here, an index of ~1 would indicate homozygous/biallelic *SDHC*me, and ~0.5 would correspond to heterozygous/monoallelic methylation at the *SDHC* promoter. As anticipated, hierarchical clustering of *d*SDH GISTs according to *SDHC*me index segregated the tumors into three *SDHC* promoter methylation (*SDHC*me) groups: homozygous/fully methylated ($n = 12$), heterozygous/hemimethylated ($n = 7$), and negative ($n = 40$) (Fig. 1C and fig. S5). All 12 homozygous *SDHC*me GISTs were from female *SDHx*-WT patients and included five of eight Carney triad cases (Fig. 1C and fig. S5). Hemimethylation encompassed four GISTs with *SDHC* heterozygous mutation (Fig. 1C and fig. S5); moreover, by genotyping and/or array comparative genomic hybridization (aCGH), these four tumors had no evidence of *SDHC* LOH, consistent with a heterozygous mutant tumor with the second hit by promoter hypermethylation (Table 1 and fig. S2); the phenomenon of second hit *SDHC* promoter methylation/silencing of the wild-type (WT) allele in heterozygous *SDHC*-mutant GIST has been previously reported (17). Three of seven hemimethylated *SDHC*me GISTs in our study were *SDHx* WT and included one Carney triad patient.

Promoter methylation of pathogenicity genes in fragile X and Lynch syndromes often stems from genomic anomalies proximal to *FMR1* and *MSH2,* respectively (20, 21). Thus, we performed deep sequencing of 12 *SDHC*me GISTs for mutations within a 130-kbp window encompassing *SDHC* and including its promoter and flanking genomic sequence. This effort did not reveal any recognizable recurrent genomic aberrations in the tumors. For completeness, additional GIST pathogenicity genes, including *KIT, PDGFRA, BRAF,* and *NF1* [four genes more typically associated with non-*d*SDH GIST (7)], were sequenced and found to lack germline or somatic mutation in these *SDHx*-WT *d*SDH GISTs. Thus, on the basis of the absence of identified genomic aberration, *SDHC* promoter methylation in GIST is consistent with primary epimutation, although future discovery of a molecular mechanism may favor reclassification as secondary epimutation. No *SDHA* ($n = 22$), *SDHB* ($n = 12$), or *SDHD* ($n = 1$) mutants had *SDHC*me (fig. S3). Among the *SDHC*me-negative cases were two *SDHC* mutants; although these tumors lacked *SDHC* promoter hemimethylation, both had second hits to *SDHC* due to chromosome 1q23 LOH encompassing *SDHC* and resulting in biallelic mutation in the tumor (Table 1 and fig. S2C).

In sum, 58 of 59 (98%) *d*SDH GISTs demonstrated *SDHx* mutation, *SDHC* promoter hypermethylation, or *SDHC* mutation plus *SDHC*me as a second hit, whereas one tumor remained *SDHx*-WT and *SDHC*me-negative (Table 1). As in all *SDHx*-WT cases in our

study, this case does not harbor *SDHA, SDHB,* or *SDHD* promoter hypermethylation (fig. S3) and does not have tumor LOH that would point to overlying genetic mutation.

Regarding Carney triad, six of eight tumors with this clinical annotation demonstrate *SDHC*me (five homozygous and one hemimethylated; fig. S5), but the tumors from two patients designated Carney triad (due to co-occurrence of *d*SDH GIST and pulmonary chondroma) were found to harbor *SDHA* mutation and negative *SDHC*me (Table 1, Fig. 1C, and figs. S3 and S5). We interpret the data as most consistent with alternative *SDHC*me and *SDHx*-mutant molecular subtypes of Carney triad as defined by anatomic criteria. Although some investigators may reclassify patients with GIST and pulmonary chondroma as not having Carney triad owing to the finding of *SDHA* mutation, others may favor keeping the Carney triad diagnosis on the basis of anatomical-pathology criteria. Why Carney triad shows a greater correlation with *SDHC* epimutation than *SDHx* mutation ($P = 0.0025$) and whether the Carney triad definition should change from purely morphologic criteria to incorporate *SDHC* epimutation status are interesting topics for future study. Because currently there is no diagnostic marker specific for Carney triad, longitudinal observation of *d*SDH GIST patients may demonstrate utility of *SDHC*me as a biomarker of increased risk for paraganglioma and/or pulmonary chondroma.

SDHx-WT GIST patients, including those with and without Carney triad manifestations, were significantly younger than mutant counterparts (average age, 17 years versus 29 years; $P = 0.003$; Table 1). *SDHx*-WT patients with Carney triad manifestations were not significantly older at the time of initial GIST diagnosis than those without manifestations (average age, 19 years versus 16 years; $P = 0.57$; Table 1).

None of the *SDHC*-epimutant GISTs in our study demonstrated hypermethylated *SDHA, SDHB,* or *SDHD* promoters by 450K methylation microarrays (Fig. 1A and fig. S3), which target multiple CpG sites in each respective promoter. In addition, none of the *d*SDH GISTs we studied, including *SDHx*-mutant and *SDHx*-WT, had large contiguous deletions on chromosome 1q (fig. S2H). Stand-alone *SDHC* epimutation in *SDHx*-WT GIST in our study contrasts with a recently proposed molecular triad of simultaneous chromosome 1q deletion and *SDHB* and *SDHC* promoter methylation that were based on a high–cycle number (60-cycle) bisulfite polymerase chain reaction (PCR) assay applied to a series of three Carney triad GISTs (26). Therefore, it seems uncharacteristic that tumors could simultaneously harbor both *SDHB* and *SDHC* promoter hypermethylation. One case in our study (*d*SDH38) had a relatively small 8.4-kbp germline intragenic deletion in *SDHC*, identical to that previously reported in a paraganglioma (27) (known as the “Pittsburgh mutation”), with tumor LOH in the remaining allele; however, outside of relatively rare instances of germline *SDHC* intragenic deletions in patients with paraganglioma and/or GIST that then complete the mutation with LOH, there are no events in our cases that would classify as chromosome band size deletions on 1q in *d*SDH GIST (fig. S2H).

To evaluate the more generai specificity of *SDHC*me to *SDHx*-WT GIST, we analyzed 450K Infinium methylation profiles from a reference panel of more than 2300 normal and cancer tissues. We evaluated multiple project data sets from the GEO and The Cancer Genome Atlas (TCGA) databases, including non-GIST pediatric tumors; mesenchymal,

neuroectodermal, and epithelial tumors; and specimens with *SDHx, IDH1/2,* or *TET* mutations and associated with a hypermethylator epigenotype. These were evaluated for *SDHC* promoter methylation using all 11 microarray *SDHC* promoter CGI targets. Beyond the *SDHx*-WT and *SDHC*-mutant GISTs in our study, we identified no cancers in GEO with a hypermethylated *SDHC* promoter (Fig. 1D). One cancer specimen out of multiple TCGA data sets—an instance of papillary renal carcinoma (1 of 226 total papillary kidney cancers with methylation array data)—was found to have hemimethylated *SDHC*me (specimen ID: TCGA-F9-A8NY-01A-11D-A369–05; fig. S6). Although SDH-deficient renal tumors have been recently described, they do not typically have papillary morphology, making this particular case even more of an anomaly. Beyond such rare cases, the absence of *SDHC* promoter hypermethylation in reference tissues suggests that, in both normal and tumor tissues, the *SDHC* gene promoter is strongly protected against methylation, and heightens its pathobiological relevance in *d*SDH GIST. Furthermore, the tumor-specific convergence in *d*SDH GIST of mutually exclusive *SDHC*me and *SDHx* mutation meets the criteria for driver epimutation as recently discussed by Sproul and Meehan (28). One feature of embryonic stem cells and induced pluripotent stem cells relative to somatic differentiated tissues and sperm is that the *SDHC* distal upstream promoter CGI becomes partially methylated (fig. S7); however, complete *SDHC* promoter hypermethylation spanning the CGI most proximal to the transcription start site (TSS) remains specific to *SDHC*-epimutant GIST (Fig. 1 and fig. S7).

SDHC silencing in *SDHC*me tumors

The connection between DNA methylation and gene expression was evaluated by profiling 20 FFPE *d*SDH GISTs with Affymetrix U133P2 arrays, containing 54,675 probe sets. Whole-genome expression analysis of 7 *SDHx*-WT and 13 *SDHx* mutants identified 4 (of 54,675 total) probe sets with significantly decreased expression ($q < 0.05$) in *SDHx*-WT *d*SDH GIST (Fig. 1A). These probe sets all map to the *SDHC* locus, have the *SDHC* promoter as the nearest transcription start site, and have an average 4.3-fold reduced expression in *SDHx*-WT tumors (Figs. 1A and 2). In addition to these *SDHC* probe sets, two other *SDHC* probe sets showed hypoexpression with *q* values between 0.05 and 0.25. No gene expression differences other than *SDHC* met the significance threshold in the *SDHx*-WT versus *SDHx*-mutant comparison (Fig. 1A and fig. S4). *SDHC* expression silencing was independently validated using an alternative RNA amplification and labeling protocol before array hybridization (fig. S8) and by quantitative reverse transcription PCR (RT-PCR) (fig. S8). Thus, three independent gene expression profiling methods validated *SDHC* silencing in *SDHx*-WT GIST. Additional analyses of sex chromosome–linked gene expression further demonstrated the biological legitimacy of the combination of samples and expression array analyses (fig. S8).

The Janus plot demonstrates reciprocal epimutation and expression silencing of *SDHC* within the *SDHx*-WT tumor group (Fig. 1A), and hierarchical clustering according to *SDHC* expression perfectly segregated *SDHC*me-positive ($n = 8$) and *SDHC*me-negative ($n = 12$) samples (Fig. 2A), clearly demonstrating the coupling of the epimutation with gene silencing within individual specimens. Similarly, this *SDHC* expression-based hierarchical clustering nearly perfectly segregated specimens according to *SDHx*-WT versus *SDHx*-

mutant status, with the exception of a heterozygous *SDHC* mutant with promoter methylation as the second hit (Fig. 2A), whose reduced *SDHC* expression is consistent with gene inactivation via tandem monoallelic silencing and mutation.

Expression microarray data were available for three cases with the clinical annotation of Carney triad (Fig. 2A): an *SDHx*-WT case demonstrated homozygous *SDHC*me and expression silencing, and two *SDHA*-mutant cases were *SDHC*me-negative with conserved *SDHC* expression. Thus, as we found for *SDHC* promoter methylation, we identified molecular heterogeneity in the transcription of *SDHC* within patients classified as Carney triad. Our results suggest that *SDHC* epimutation—evidenced by promoter methylation and gene expression silencing—is common among Carney triad GISTs. However, it is important to note that some patients with a morphology-based Carney triad diagnosis may have *SDHx* mutation, negative *SDHC*me, and maintenance of *SDHC* transcription, and that most GIST cases with *SDHC*me and silencing are not associated with Carney triad at the time of diagnosis. Although case studies have reported *SDHC* promoter methylation (coupled to other changes not evident in our series, such as *SDHB* promoter methylation and large contiguous deletions on chromosome 1q) in selected Carney triad patients (26), analysis of 59 *d*SDH GISTs unselected for Carney triad status has revealed *SDHC*me as a frequent recurrent anomaly that is neither perfectly sensitive nor specific for Carney triad. Because Carney triad is a post hoc diagnosis based on the emergence of a spectrum of tumors over the lifetime of a patient, longitudinal follow-up is necessary to establish the prognostic specificity of GIST *SDHC* epimutation status for subsequent development of Carney triad sequelae.

Mosaic constitutional *SDHC* epimutation in patients with *SDHC*-epimutant GIST

Epimutation may be encountered soma-wide in patients with disorders like fragile X and Lynch syndromes. We tested blood and saliva from *SDHx*-WT GIST patients for constitutional *SDHC* epimutation, the manifestations of which could provide insight into the developmental timing/establishment of the epimutant DNA methylation mark. Whole blood from *SDHx*-WT GIST patients showed a modest but significant 2.7% mean elevation in *SDHC* promoter methylation versus the *SDHx*-mutant group ($P = 0.003$, Fig. 3). *SDHC* promoter methylation was further evident in saliva (fig. S9), which like blood showed a significant ($P = 0.018$) mean 2.4% elevation of *SDHC* methylation. The blood and saliva of several *SDHC*-epimutant GIST patients had up to 10% elevation in *SDHC* promoter methylation (fig. S9).

DISCUSSION

Previous studies have shown that *d*SDH GISTs are collectively characterized by genome-wide hypermethylation and low cytogenetic complexity (1, 7); the absence of both *SDHx* coding mutations and LOH in many cases left the SDH-deficient tumor phenotype unexplained.

In the current study, we demonstrate that *SDHx*-WT GISTs, including several from patients with Carney triad, commonly arise from *SDHC* epimutation, evidenced by highly focal *SDHC* promoter CGI hypermethylation and transcriptional silencing. *SDHC* epimutation

was the only distinction between *SDHx*-WT and *SDHx*-mutant GIST by genome-wide DNA methylation and expression profiling and was mutually exclusive of *SDHx* mutation, with the notable exception of *SDHC* heterozygous mutant tumors with silencing of the second allele by *SDHC* promoter methylation. *SDHC* epimutation does not appear to be a polymorphism or passenger epiallele, because a reference panel of more than 2300 benign and tumor tissues, including malignancies with a hypermethylator epigenotype, show conservation of an unmethylated *SDHC* promoter, indicating strong protection from methylation and silencing, perhaps as expected for a gene encoding an essential mitochondrial protein. Regarding a recently proposed molecular triad of hypermethylation of both *SDHB* and *SDHC* promoters coupled with 1q deletion as a mechanism of SDH deficiency in Carney triad tumors (19, 28), we found no instances of simultaneous *SDHC* and *SDHx* comethylation and no cases with large chromosome 1q deletion. Instead, *SDHC* promoter methylation and/or gene expression silencing alone is pathognomonic for an SDH-deficient tumor. These results establish *SDHC* epimutation as the molecular pathologic basis for disabling the SDH complex in most of *SDHx*-WT GIST patients, encompassing those with Carney triad.

Blood and saliva from patients with *SDHC*-epimutant GIST manifest detectable but sub-hemimethylated levels of *SDHC* epimutation as well. Although distinct from those Lynch syndrome patients with soma-wide *MLH1* hemimethylation (20), low to modest levels of statistically significant *SDHC* methylation in patients with *SDHC*-epimutant GIST are reminiscent of mosaic low-level *MLH1* methylation (2 to 5%) in the blood of other Lynch patients (20). Overall, we interpret *SDHC* hypermethylation in the blood and saliva of *SDHx*-WT/*SDHC*-epimutant GIST patients to be biologically relevant and consistent with a mosaic constitutional epimutation that is clonally expanded in tumor cells; moreover, this somatic mosaicism is consistent with postzygotic *SDHC* promoter methylation reprogramming. Future studies are required to explore and further validate the manifestations of *SDHC* epimutation mosaicism in the soma of these patients. Such mosaicism in the soma is consistent with a postzygotic onset of epimutation, rather than germline inheritance, which would be expected to result in soma-wide *SDHC* hemimethylation, unless partially erased in somatic lineages. In either case, the resulting mosaicism points to a process of *SDHC* reprogramming during early development, which is then maintained so as to be detectable in blood and saliva later in life. Methylation data from additional constitutional anatomic sites from our patients are needed to further evalúate the extent of somatic mosaicism. More generally, the finding of elevated *SDHC* promoter methylation in the soma of *SDHx*-WT GIST patients highlights an emerging need in the epimutation field, namely, a large number of methylomes from saliva and other fluids to establish reference values for gene-specific methylation.

The finding of *SDHC* epimutation is important for several reasons. First, in the clinical genetic evaluation of GIST patients, our data indicate that *SDHC* epimutation frequency is comparable to *SDHx* coding sequence mutation and should be considered in *d*SDH GIST cases, particularly those that prove *SDHx*-WT. It is reasonable to hypothesize that individuals who present with an *SDHC*-epimutant GIST may be at greater risk for additional tumors, including paraganglioma and pulmonary chondroma. The identification of *SDHC* epimutation raises the possibility that demethylating agents such as decitabine could restore

SDHC expression and SDH function in *SDHx*-WT GISTs, which currently lack targeted chemotherapy. Finally, the discovery of *SDHC* epimutation now provides a unifying explanation for the pathogenesis of almost all cases of *d*SDH/methyl-divergent GIST, where loss of SDH function arises through either mutation or epimutation.

For now, detection of *SDHC* epimutation in surgical pathology specimens will require DNA methylation and/or gene expression analysis because presently there are no published methods for SDHC protein immunohistochemistry on fixed tissue, and we have attempted but so far were not able to optimize such an assay. At the same time, whole genome expression and DNA methylation profiling proved technically feasible and successful as in this study, which is encouraging for finding pathogenicity genes in rare tumor types or archival collections where only FFPE material may be available.

The rarity of trans-generational heritability of Carney triad (29), coupled with homozygous tumor *SDHC* epimutation without LOH in *SDHx*-WT GIST patients, raises the possibility of primary/de novo *SDHC* epimutation. A clue to the mechanism of *SDHC* silencing may be that homozygous *SDHC*me GISTs in our study arose only in females, implicating a potential role for sex chromosome or hormone biology in the mechanism of *SDHC* epimutation. The ability to positively identify *SDHC*-epimutant cases without awaiting the various Carney triad manifestations will enable future studies to test mechanistic hypotheses for this phenomenon.

MATERIALS AND METHODS

Study design

Fifty-nine cases from the NIH GIST clinic were identified and included in this study on the basis of molecular and pathologic demonstration of SDH deficiency. The overall goal of the study was to elucidate the molecular mechanism of SDH deficiency in GIST, particularly in *SDHx*-WT cases. Molecular profiling assays were adapted to archival FFPE surgical pathology specimens, and included NGS, Illumina 450K methylation microarray profiling, and Affymetrix gene expression microarray profiling.

Specimens and annotations

FFPE tumor tissues from 59 distinct NIH GIST clinic cases were tested. All cases received histopathologic diagnosis including immunohistochemistry for SDHA and SDHB protein expression where feasible [National Cancer Institute (NCI) Laboratory of Pathology]; only SDH-disabled tumor cases as evidenced by SDH-negative immunophenotype and/or hypermethylation epigenomic signature [methyl-divergent signature (7)] were included in the study. Malignant cell fraction in tumor tissue DNA extracts was empirically measured using the MDI as follows: the top 100 hypermethylated targets in *d*SDH GIST were identified by *t*-test comparison to *KIT*-mutant/SDHB$^+$ immunophenotype tumors from GEO data set GSE343877. In *d*SDH GIST, these 100 CpG targets approach methylation β values of 1.0, versus 0.0 in KIT-mutant/SDHB$^+$ GIST, indicative of biallelic/homozygous de novo methylation in the former (fig. S1). The MDI was calculated as the average β value of these

100 targets and termed MDI_{100}, the empirically measured malignant cellularity of tumor tissue DNA extracts (Table 1).

SDHx mutation analysis

Cases received CLIA-certified laboratory testing for coding sequence mutations in *SDHA, SDHB, SDHC, SDHD, KIT, PDGFRA, BRAF,* and *NF1* genes [OncoVar-GIST assay, NCI Clinical Molecular Profling Core (CMPC)]. The mean read depth for targeted gene coding sequences was >100×. Sequence reads were aligned with Burrows-Wheeler Aligner (BWA), and variants were called by mpileup and by visual inspection of alignments in Integrated Genome Viewer (IGV). Cases were assayed for genomic copy number aberrations and copy-neutral LOH with the Illumina FFPE CytoSNP assay after DNA treatment with FFPE restoration solution (Illumina) (Table 1 and fig. S2). Tumor genotyping microarray data were visualized with Nexus software (Biodiscovery Inc.). Cases were thereby annotated as *SDHx*-mutant versus *SDHx*-WT for subsequent statistical group comparisons. Additional case annotations included patient age, sex, and diagnosis of Carney triad (Table 1). The diagnosis of Carney triad was provided by treating physicians, and required clinical evidence of pulmonary chondroma in addition to GIST.

DNA methylation profiling

DNA extraction and genome-wide DNA methylation profiling by Illumina 450K Infinium assay were performed as previously described (7). Briefy, microdissected FFPE tissue (paraffin block needle core or glass slide razor scrape) was lysed in a cocktail containing mineral oil (for deparaffmization), proteinase K, and ATL lysis buffer (Qiagen), and resultant lysates were filter-purified by Qiagen DNA enrichment columns. Purified DNAs were treated with FFPE DNA restoration solution (Illumina) and then analyzed with the standard protocol Illumina 450K methylation beadarray assay.

Gene expression analysis

Total RNA was extracted from 0.6- to 1.0-mm FFPE tissue cores (paraffin block needle core or glass slide razor scrape) with the RNeasy FFPE Kit (Qiagen) according to the manufacturer's instructions. RNA quantity and purity were determined with a NanoDrop spectrophotometer (ND-1000, Thermo Scientific). RNA integrity was evaluated with the Bioanalyzer RNA 6000 Nano Kit (Agilent). One hundred nanograms of total RNA sample was converted to complementary DNA (cDNA) and SPIA-amplified with the Ovation FFPE WTA System (NuGEN) according to the manufacturer's instructions. SPIA-amplified cDNA was purified with the Agencourt RNAClean XP Kit (Beckman Coulter Genomics) according to the Ovation FFPE WTA System supplementary protocol. Purified cDNA was quantitated with a NanoDrop spectrophotometer. After quantitation, 4 to 5 μg of purified cDNA sample were subjected to fragmentation and biotin labeling with the Encore Biotin Module (NuGEN) according to the manufacturer's instructions. An aliquot of unfragmented and fragmented cDNA was evaluated for product size with the RNA 6000 Nano Assay. A sample hybridization cocktail, consisting of the biotin-labeled fragmented sample, hybridization controls, and hybridization buffer, was prepared according to Encore Biotin Module instructions for standard array format. The sample hybridization cocktail was applied to a GeneChip Human Genome U133 Plus 2.0 array (Affymetrix) and hybridized for 18 hours at

45°C with rotation in an Affymetrix GeneChip Hybridization Oven. The following day, the array “wash and stain” procedure was performed with the automated Affymetrix GeneChip Fluidics Station 450 and fluidics script FS450–0004. The arrays were scanned with the Affymetrix GeneChip Scanner 3000 7G.

As an alternative to and validation of Nugen-derived gene expression profiles, RNAs extracted from FFPE tissues were amplified with the SensationPlus FFPE Amplification and 3′ IVT Labeling Kit (Affymetrix) and hybridized to GeneChip Human Genome U133 Plus 2.0 Array (Afïymetrix) expression arrays (fig. S7). Briefly, according to the manufacturer’s protocol, 200 ng of total RNA sample was subjected to one round of cDNA synthesis followed by sense RNA amplification, a second round of cDNA synthesis, fragmentation, and biotin labeling. Subsequent array hybridization and processing steps were the same as described above for Nugen-amplified RNAs. *SDHC* expression silencing was also validated by quantitative RT-PCR (fig. S8) as follows. cDNA was generated from FFPE-extracted total RNA with the Message*BOOSTER* Whole Transcriptome cDNA Synthesis Kit for quantitative PCR (Epicentre, cat. no. MBWT80510) according to the manufacturer’s instructions. *SDHC* primers, tccagaccggaacccaagat (forward) and cgaccaacgtgtctcagcaa (reverse), were used to amplify a 50-bp spliced transcript; the *ACTB* PrimePCR SYBR Green assay (Bio-Rad) was amplified as an internal control for expression level normalization. SsoAdvanced Universal SYBR Green Supermix (Bio-Rad, cat. no. 172–5270) was used to amplify *SDHC* and *ACTB* cDNA targets according to the manufacturer’s protocol with the CFX96 instrument (Bio-Rad), operated by CFX Manager software. Cycling conditions included a polymerase activation step of 98°C for 2 min and 40 cycles of 98°C for 2 s and annealing/extension at 60°C for 5 s with melt curve analysis from 65° to 95°C in 0.5°C increments.

Deep sequencing of SDHC and flanking regions

A 130-kb window centered on the *SDHC* gene, including its promoter and flanking genes (hg19 chr1:161246130–161408301), was targeted for deep sequencing in *SDHC*-epimutant cases using tiling custom-capture baits applied to GIST gDNA libraries constructed according to standard protocols (Illumina Tru-Seq). The custom capture baits consisted of biotinylated probes derived by Klenow amplification of *SDHC*-containing BAC (bacterial artificial chromosome) clone RP11–122G18. Posthybridization libraries were sequenced on the MiSeq to an average >500× coverage.

Microarray processing, normalization, and statistical analyses

Infinium 450K methylation array image files (.idat) were imported to GenomeStudio software (Illumina Inc.), using the methylation module; Cy3/Cy5 color channel normalization and background subtraction were performed according to the manufacturer’s instructions; sample methylation β values (which approximate the percent methylation at genomic CpG loci) were computed with the GenomeStudio methylation analysis function, and b values were exported from GenomeStudio for subsequent statistical analyses and visualization with Qlucore Omics Explorer v.3 software (QOE). For each patient’s blood or saliva samples, target methylation β values were calculated from 450K methylation array data using the group methylation profile in GenomeStudio; this function computes the

average target methylation β value for any sample technical replicates. Tumor *SDHC*me zygosity and blood and saliva *SDHC*me levels were based on the average β value across *SDHC* promoter CpG targets mapping to the TSS-proximal CGI (cg00576014, cg01931502, cg11221265, cg12036621, and cg17496230). Normalized gene expression profiles were generated from Affymetrix .CEL files by importing .CEL files into QOE and selecting the RMA (robust multi-array average) normalization algorithm. The QOE QC report tool was used to verify the quality of individual expression arrays and exclude outliers. Samples were annotated into *SDHx*-mutant versus *SDHx*-WT groups as described above (*SDHx* mutation analysis), and the between-group significance of each 450K methylation CpG target variable or U133P2 probe set variable [*q* value, a false discovery rate-corrected *P* value (30)] was computed in QOE, which uses a *t* test for two-group comparisons. CpG target and expression probe set variables were annotated for hg19 genomic map position and closest gene, using microarray manufacturer annotations and probe sequence information. $-\text{Log}_{10}(q)$ methylation (upward facing hypermethylation) and $\log_{10}(q)$ gene expression (downward facing hypoexpression) were plotted as a function of genomic map position using R (Fig. 1A). The validity of gene expression microarray statistical approaches was verified by analysis of sex-linked gene expression, which showed data consistent with specimen male/female sex annotation (fig. S7).

Supplementary Material

Refer to Web version on PubMed Central for supplementary material.

Acknowledgments

Funding: We thank the Life Raft Group and the Intramural Research Program of NIH, NCI, Center for Cancer Research, for funding this study.

REFERENCES AND NOTES

1. Belinsky MG, Rink L, von Mehren M, Succinate dehydrogenase deficiency in pediatric and adult gastrointestinal stromal tumors. Front. Oncol 3, 117 (2013). [PubMed: 23730622]
2. Gill AJ, Succinate dehydrogenase (SDH) and mitochondrial driven neoplasia. Pathology 44, 285–292 (2012). [PubMed: 22544211]
3. Pollard PJ, Brière JJ, Alam NA, Barwell J, Barclay E, Wortham NC, Hunt T, Mitchell M, Olpin S, Moat SJ, Hargreaves IP, Heales SJ, Chung YL, Griffiths JR, Dalgleish A, McGrath JA, Gleeson MJ, Hodgson SV, Poulsom R, Rustin P, Tomlinson IP, Accumulation of Krebs cycle intermediates and over-expression of HIF1α in tumours which result from germline FH and SDH mutations. Hum. Mol. Genet 14, 2231–2239 (2005). [PubMed: 15987702]
4. Selak MA, Armour SM, MacKenzie ED, Boulahbel H, Watson DG, Mansfield KD, Pan Y, Simon MC, Thompson CB, Gottlieb E, Succinate links TCA cycle dysfunction to oncogenesis by inhibiting HIF-α prolyl hydroxylase. Cancer Cell 7, 77–85 (2005). [PubMed: 15652751]
5. MacKenzie ED, Selak MA, Tennant DA, Payne LJ, Crosby S, Frederiksen CM, Watson DG, Gottlieb E, Cell-permeating α-ketoglutarate derivatives alleviate pseudohypoxia in succinate dehydrogenase-deficient cells. Mol. Cell. Biol 27, 3282–3289 (2007). [PubMed: 17325041]
6. Cervera AM, Bayley JP, Devilee P, McCreath KJ, Inhibition ofsuccinate dehydrogenase dysregulates histone modification in mammalian cells. Mol. Cancer 8, 89 (2009). [PubMed: 19849834]
7. Killian JK, Kim SY, Miettinen M, Smith C, Merino M, Tsokos M, Quezado M, Smith WI Jr., Jahromi MS, Xekouki P, Szarek E, Walker RL, Lasota J, Raffeld M, Klotzle B, Wang Z, Jones L, Zhu Y, Wang Y, Waterfall JJ, O'Sullivan MJ, Bibikova M, Pacak K, Stratakis C, Janeway KA,

Schiffman JD, Fan JB, Helman L, Meltzer PS, Succinate dehydrogenase mutation underlies global epigenomic divergence in gastrointestinal stromal tumor. Cancer Discov 3, 648–657 (2013). [PubMed: 23550148]

8. Waterfall JJ, Killian JK, Meltzer PS, The role of mutation of metabolism-related genes in genomic hypermethylation. Biochem. Biophys. Res. Commun 455, 16–23 (2014). [PubMed: 25111818]
9. Letouzé E, Martinelli C, Loriot C, Burnichon N, Abermil N, Ottolenghi C, Janin M, Menara M, Nguyen AT, Benit P, Buffet A, Marcaillou C, Bertherat J, Amar L, Rustin P, De Reyniès A, Gimenez-Roqueplo AP, Favier J, SDH mutations establish a hypermethylator phenotype in paraganglioma. Cancer Cell 23, 739–752 (2013). [PubMed: 23707781]
10. Xiao M, Yang H, Xu W, Ma S, Lin H, Zhu H, Liu L, Liu Y, Yang C, Xu Y, Zhao S, Ye D, Xiong Y, Guan KL, Inhibition of α-KG-dependent histone and DNA demethylases by fumarate and succinate that are accumulated in mutations of FH and SDH tumor suppressors. Genes Dev 26, 1326–1338 (2012). [PubMed: 22677546]
11. Noushmehr H, Weisenberger DJ, Diefes K, Phillips HS, Pujara K, Berman BP, Pan F, Pelloski CE, Sulman EP, Bhat KP, Verhaak RG, Hoadley KA, Hayes DN, Perou CM, Schmidt HK, Ding L, Wilson RK, Van Den Berg D, Shen H, Bengtsson H, Neuvial P, Cope LM, Buckley J, Herman JG, Baylin SB, Laird PW, Aldape K; Cancer Genome Atlas Research Network, Identification of a CpG island methylator phenotype that defines a distinct subgroup of glioma. Cancer Cell 17, 510–522 (2010). [PubMed: 20399149]
12. Figueroa ME, Abdel-Wahab O, Lu C, Ward PS, Patel J, Shih A, Li Y, Bhagwat N, Vasanthakumar A, Fernandez HF, Tallman MS, Sun Z, Wolniak K, Peeters JK, Liu W, Choe SE, Fantin VR, Paietta E, Löwenberg B, Licht JD, Godley LA, Delwel R, Valk PJ, Thompson CB, Levine RL, Melnick A, Leukemic IDH1 and IDH2 mutations result in a hypermethylation phenotype, disrupt TET2 function, and impair hematopoietic differentiation. Cancer Cell 18, 553–567 (2010). [PubMed: 21130701]
13. Pansuriya TC, van Eijk R, d'Adamo P, A van Ruler M, L Kuijjer M, Oosting J, Cleton-Jansen AM, van Oosterwijk JG, Verbeke SL, Meijer D, van Wezel T, Nord KH, Sangiorgi L, Toker B, Liegl-Atzwanger B, San-Julian M, Sciot R, Limaye N, Kindblom LG, Daugaard S, Godfraind C, Boon LM, Vikkula M, Kurek KC, Szuhai K, French PJ, Bovée JV, Somatic mosaic IDH1 and IDH2 mutations are associated with enchondroma and spindle cell hemangioma in Ollier disease and Maffucci syndrome. Nat. Genet 43, 1256–1261 (2011). [PubMed: 22057234]
14. Agaram NP, Laquaglia MP, Ustun B,Guo T, Wong GC, Socci ND, Maki RG, DeMatteo RP, Besmer P, Antonescu CR, Molecular characterization of pediatric gastrointestinal stromal tumors. Clin. Cancer Res 14, 3204–3215 (2008). [PubMed: 18483389]
15. Prakash S, Sarran L, Socci N, DeMatteo RP, Eisenstat J, Greco AM, Maki RG, Wexler LH, LaQuaglia MP, Besmer P, Antonescu CR, Gastrointestinal stromal tumors in children and young adults: A clinicopathologic, molecular, and genomic study of 15 cases and review ofthe literature. J. Pediatr. Hematol. Oncol 27, 179–187 (2005). [PubMed: 15838387]
16. Lasota J, Wang Z, Kim SY, Helman L, Miettinen M, Expression of the receptor for type I insulin-like growth factor (IGF1R) in gastrointestinal stromal tumors: An immunohistochemical study of 1078 cases with diagnostic and therapeutic implications. Am. J. Surg. Pathol 37, 114–119 (2013). [PubMed: 22892600]
17. Belinsky MG, Rink L, Flieder DB, Jahromi MS, Schiffman JD, Godwin AK, Mehren M, Overexpression of insulin-like growth factor 1 receptor and frequent mutational inactivation of SDHA in wild-type SDHB-negative gastrointestinal stromal tumors. Genes Chromosomes Cancer 52, 214–224 (2013). [PubMed: 23109135]
18. Carney JA, Carney triad. Front. Horm. Res 41, 92–110 (2013). [PubMed: 23652673]
19. Matyakhina L, Bei TA, McWhinney SR, Pasini B, Cameron S, Gunawan B, Stergiopoulos SG, Boikos S, Muchow M, Dutra A, Pak E, Campo E, Cid MC, Gomez F, Gaillard RC, Assie G, Fuzesi L, Baysal BE, Eng C, Carney JA, Stratakis CA, Genetics of Carney triad: Recurrent losses at chromosome 1 but lack of germline mutations in genes associated with paragangliomas and gastrointestinal stromal tumors. J. Clin. Endocrinol. Metab 92, 2938–2943 (2007). [PubMed: 17535989]
20. Hitchins MP, The role of epigenetics in Lynch syndrome. Fam. Cancer 12, 189–205 (2013). [PubMed: 23462881]

21. Colak D, Zaninovic N, Cohen MS, Rosenwaks Z, Yang WY, Gerhardt J, Disney MD, Jaffrey SR, Promoter-bound trinucleotide repeat mRNA drives epigenetic silencing in fragile X syndrome. Science 343, 1002–1005 (2014). [PubMed: 24578575]
22. Miettinen M, Wang ZF, Sarlomo-Rikala M, Osuch C, Rutkowski P, Lasota J, Succinate dehydrogenase-deficient GISTs: A clinicopathologic, immunohistochemical, and molecular genetic study of 66 gastric GISTs with predilection to young age. Am. J. Surg. Pathol 35, 1712–1721 (2011). [PubMed: 21997692]
23. Killian JK, Bilke S,Davis S, Walker RL, Jaeger E, Killian MS,Waterfall JJ, Bibikova M,Fan JB, Smith WI Jr., P. S. Meltzer, A methyl-deviator epigenotype of estrogen receptor-positive breast carcinoma is associated with malignant biology. Am.J. Pathol 179, 55–65 (2011). [PubMed: 21641572]
24. Knudson AG Jr., Mutation and cancer: Statistica! study of retinoblastoma. Proc. Natl. Acad. Sci. U.S.A 68, 820–823 (1971). [PubMed: 5279523]
25. Miettinen M, Killian JK, Wang ZF, Lasota J, Lau C, Jones L, Walker R, Pineda M, Zhu YJ, Kim SY, Helman L, Meltzer P, Immunohistochemical loss of succinate dehydrogenase subunit A (SDHA) in gastrointestinal stromal tumors (GISTs) signals SDHA germline mutation. Am. J. Surg. Pathol 37, 234–240 (2013). [PubMed: 23282968]
26. Haller F, Moskalev EA, Faucz FR, Barthelmeß S, Wiemann S, Bieg M, Assie G, Bertherat J, Schaefer IM, Otto C, Rattenberry E, Maher ER, Ströbel P, Werner M, A Carney J, A Hartmann CA Stratakis, A. Agaimy, Aberrant DNA hypermethylation of SDHC: A novel mechanism of tumor development in Carney triad. Endocr. Relat. Cancer 21, 567–577 (2014). [PubMed: 24859990]
27. Baysal BE, Willett-Brozick JE, Filho PA, Lawrence EC, Myers EN, Ferrell RE, An Alumediated partial SDHC deletion causes familial and sporadic paraganglioma. J. Med. Genet 41, 703–709 (2004). [PubMed: 15342702]
28. Sproul D, Meehan RR, Genomic insights into cancer-associated aberrant CpG island hypermethylation. Brief. Funct. Genomics 12, 174–190 (2013). [PubMed: 23341493]
29. Carney JA, Gastric stromal sarcoma, pulmonary chondroma, and extra-adrenal paraganglioma (Carney triad): Natural history, adrenocortical component, and possible familial occurrence. Mayo Clin. Proc 74, 543–552 (1999). [PubMed: 10377927]
30. Benjamini Y, Hochberg Y, Controlling the false discovery rate: A practical and powerful approach to multiple testing. J. R. Stat. Soc. Series B Stat. Methodol 57, 289–300 (1995).

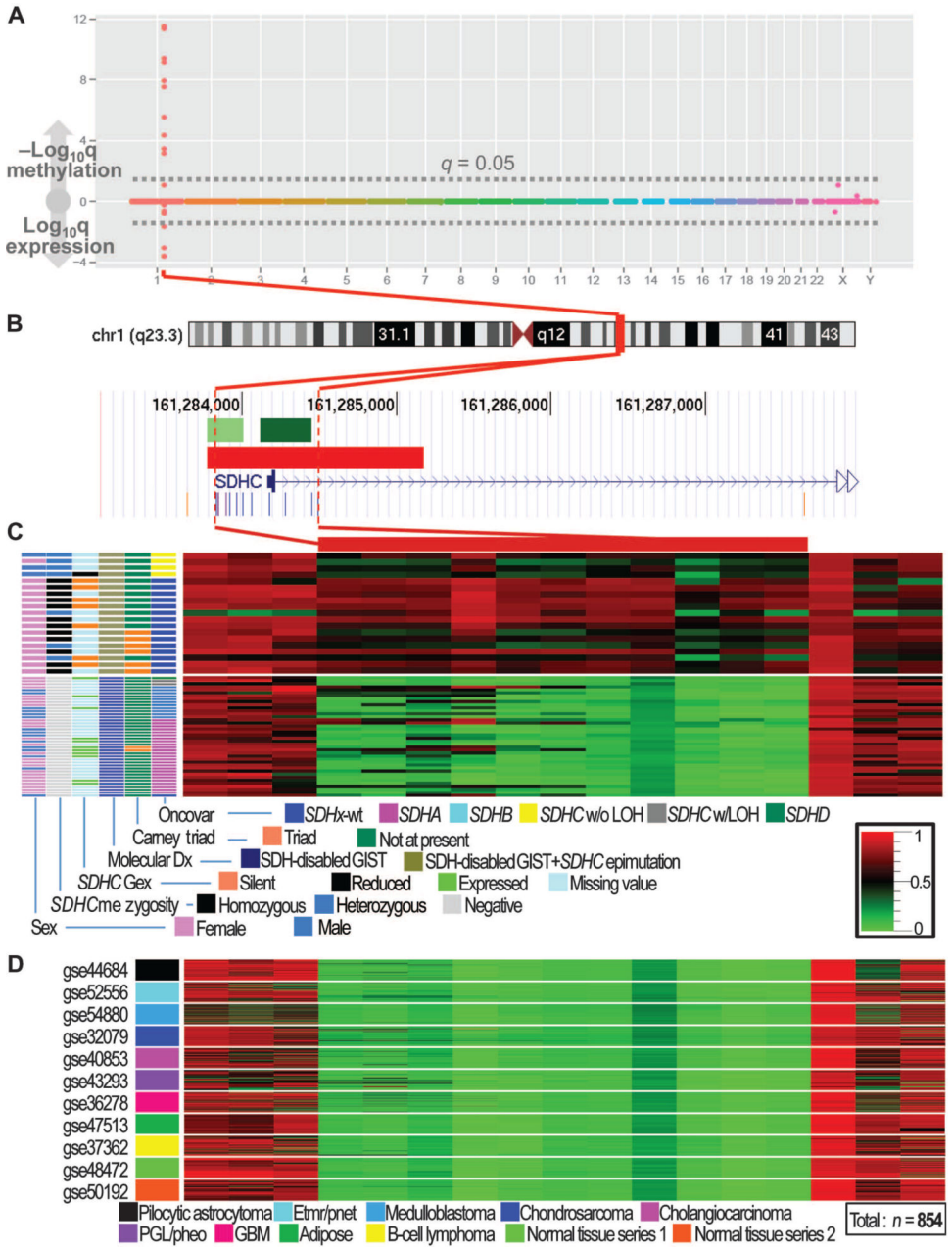

Fig. 1. *SDHC* epimutation in *SDHx*-WT *d*SDH GIST.

(A) Janus plot showing upward facing CpG target hypermethylation ($-\log_{10}q$) and downward facing gene probe set hypoexpression ($\log_{10}q$) in *SDHx-WT* versus *SDHx*-mutant GIST, calculated from *t*-test comparison of genome-wide methylation and expression profiles, plotted on genome coordinates. *q*-value significance thresholds ($q = 0.05$, gray dotted lines) are indicated. (**B**) UCSC (University of California, Santa Cruz) genome browser display shows genomic position (hg19 coordinates), CGIs (green bars), *SDHC* promoter (red bar), and *SDHC* 5'UTR/exon 1 in relation to hypermethylated and hypoexpressed targets. The lower browser track shows the position of each 450K Infinium methylation CpG target in the region. (**C**) Heatmaps show methylation β values (legend at

bottom right) of the 11 significant hypermethylated Infinium 450K CpG targets spanning the *SDHC* promoter ($q < 0.05$, red bar over upper heatmap) and upstream and downstream flanking regions. *SDHCme*-positive (upper heatmap) or *SDHC*me-negative (lower heatmap) GIST samples are ordered according to *SDHx* mutation. (**D**) 450K Infinium methylation data from 854 normal and tumor reference tissues from the GEO database (project IDs shown on the left of the heatmap). ETMR/PNET, embryonal tumor with multilayer rosettes/peripheral neuroectodermal tumor; PGL/Pheo, paraganglioma/pheochromocytoma; GBM, glioblastoma multiforme.

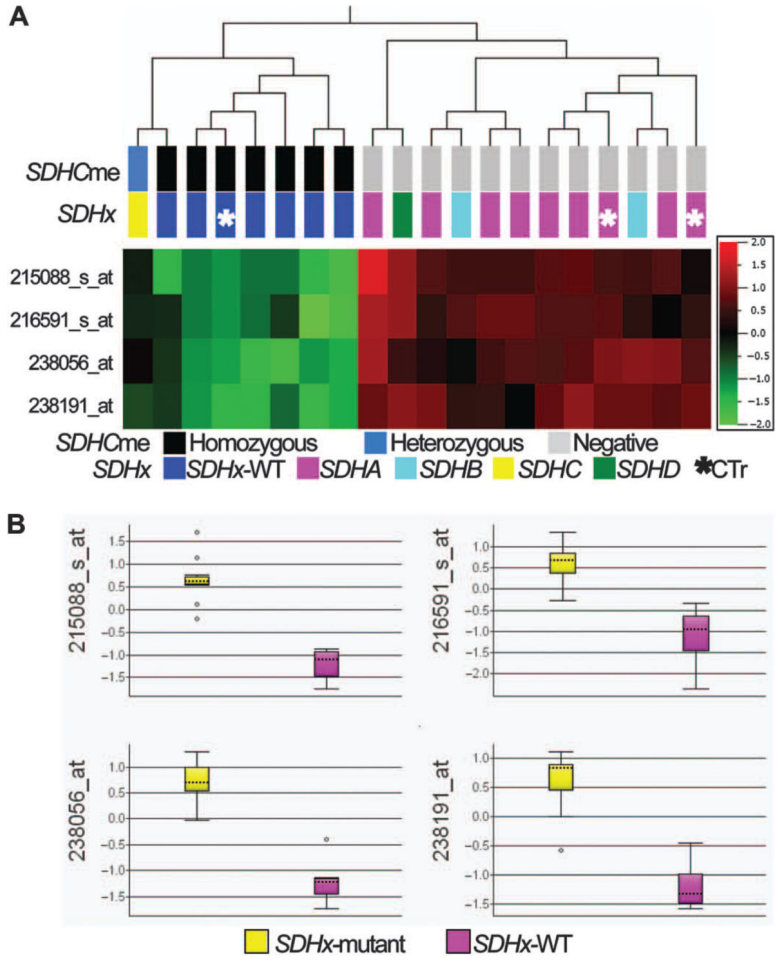

Fig. 2. *SDHC* silencing in *SDHx*-WT *d*SDH GIST.

(A) Heatmap shows the expression (legend on the right) of all probe sets identified by Affymetrix U133P2 microarrays as being significantly different between *SDHx*-mutant GIST ($n = 13$) and *SDHx-WT* GIST ($n = 7$) ($q < 0.05$). The four probe sets map to *SDHC.* CTr, Carney triad. (**B**) Boxplots of *SDHC* probe set expression demonstrate an average 4.3-fold silencing in *SDHx-WT* GIST.

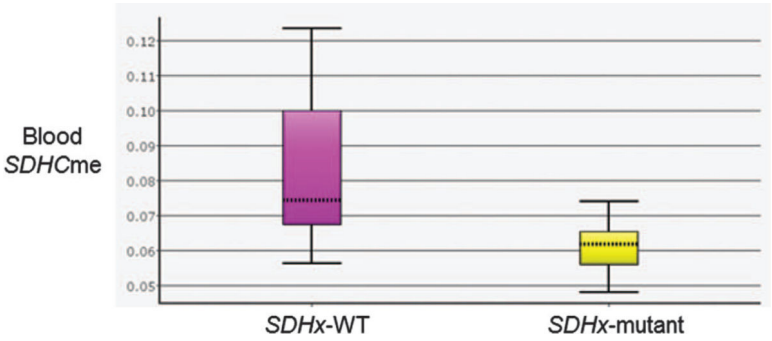

Fig. 3. *SDHC* promoter methylation in blood.

Boxplot of *SDHC* promoter methylation in blood of *SDHx-WT* ($n = 11$) and *SDHx*-mutant ($n = 14$) GIST patients shows a 2.7% mean elevation in the *SDHx-WT* group ($P = 0.003$). *SDHC* promoter methylation in blood from individual patients is shown in fig. S9.

Table 1.

Characteristics of the 59 study cases.

Case no.	Age at Dx (years)	Sex	*SDHx* mutation	Second hit	MDI_{100}	*SDHC*me zygosity
*d*SDH1	7	F	*SDHA*	Mutation	0.89	Negative
*d*SDH2	11	M	*SDHA*	NF	0.75	Negative
*d*SDH3	16	M	*SDHA*	NF	0.89	Negative
*d*SDH4	16	F	*SDHA*	Mutation	0.79	Negative
*d*SDH5	18	F	*SDHA*	NF	0.87	Negative
*d*SDH6	19	F	*SDHA*	LOH	0.65	Negative
*d*SDH7	20	F	*SDHA*	NF	0.76	Negative
*d*SDH8*	21	M	*SDHA*	LOH	0.89	Negative
*d*SDH9	21	F	*SDHA*	NF	0.77	Negative
*d*SDH10	23	F	*SDHA*	Mutation	0.86	Negative
*d*SDH11	23	M	*SDHA*	Mutation	0.74	Negative
*d*SDH12	26	F	*SDHA*	Mutation	0.66	Negative
*d*SDH13	27	F	*SDHA*	LOH	0.81	Negative
*d*SDH14	30	M	*SDHA*	LOH	0.71	Negative
*d*SDH15*	30	M	*SDHA*	NF	0.89	Negative
*d*SDH16	32	F	*SDHA*	NF	0.81	Negative
*d*SDH17	33	M	*SDHA*	Mutation	0.87	Negative
*d*SDH18	34	F	*SDHA*	LOH	0.90	Negative
*d*SDH19	35	F	*SDHA*	Mutation	0.86	Negative
*d*SDH20	39	M	*SDHA*	NF	0.85	Negative
*d*SDH21	40	F	*SDHA*	Mutation	0.75	Negative
*d*SDH22	41	F	*SDHA*	LOH	0.91	Negative
*d*SDH23	50	F	*SDHA*	LOH	0.90	Negative
*d*SDH24	55	F	*SDHA*	LOH	0.77	Negative
*d*SDH25	55	F	*SDHA*	Mutation	0.87	Negative
*d*SDH26	11	F	*SDHB*	LOH	0.91	Negative
*d*SDH27	17	M	*SDHB*	LOH	0.88	Negative
*d*SDH28	18	M	*SDHB*	LOH	0.83	Negative
*d*SDH29	19	M	*SDHB*	LOH	0.54	Negative
*d*SDH30	22	M	*SDHB*	LOH	0.69	Negative
*d*SDH31	24	M	*SDHB*	LOH	0.58	Negative
*d*SDH32	24	M	*SDHB*	LOH	0.73	Negative
*d*SDH33	33	F	*SDHB*	LOH	0.82	Negative
*d*SDH34	48	F	*SDHB*	LOH	0.71	Negative
*d*SDH35	49	F	*SDHB*	LOH	0.85	Negative
*d*SDH36	50	F	*SDHB*	LOH	0.72	Negative
*d*SDH37	20	F	*SDHC*	LOH	0.80	Negative
*d*SDH38	31	F	*SDHC*	LOH	0.82	Negative
*d*SDH39	11	M	*SDHC*	SDHC-me	0.76	Hemimethylated

Case no.	Age at Dx (years)	Sex	*SDHx* mutation	Second hit	MDI_{100}	*SDHC*me zygosity
*d*SDH40	18	M	*SDHC*	SDHC-me	0.85	Hemimethylated
*d*SDH41	19	M	*SDHC*	SDHC-me	0.77	Hemimethylated
*d*SDH42	57	F	*SDHC*	SDHC-me	0.64	Hemimethylated
*d*SDH43	38	F	*SDHD*	LOH	0.85	Negative
*d*SDH44	8	F	*SDHX* WT	NA	0.71	Hemimethylated
*d*SDH45*	8	F	*SDHX* WT	NA	0.85	Homozygous
*d*SDH46	9	F	*SDHX* WT	NA	0.78	Homozygous
*d*SDH47	10	F	*SDHX* WT	NA	0.86	Homozygous
*d*SDH48	11	F	*SDHX* WT	NA	0.87	Hemimethylated
*d*SDH49	12	F	*SDHX* WT	NA	0.82	Homozygous
*d*SDH50	12	F	*SDHX* WT	NA	0.88	Homozygous
*d*SDH51	13	F	*SDHX* WT	NA	0.84	Homozygous
*d*SDH52*	14	F	*SDHX* WT	NA	0.74	Homozygous
*d*SDH53	15	F	*SDHX* WT	NA	0.82	Homozygous
*d*SDH54*	18	F	*SDHX* WT	NA	0.70	Homozygous
*d*SDH55*	22	F	*SDHX* WT	NA	0.76	Homozygous
*d*SDH56	25	M	*SDHX* WT	NA	0.87	Negative
*d*SDH57*	26	F	*SDHX* WT	NA	0.77	Hemimethylated
*d*SDH58*	28	F	*SDHX* WT	NA	0.56	Homozygous
*d*SDH59	47	F	*SDHX* WT	NA	0.74	Homozygous

NF, none found; Dx, diagnosis; NA, not applicable.

*Carney triad.